

## Research Article

# Characterizing the Deacidification Adsorption Model of Organic Acids and Phenolic Compounds of Noni Extract Using Weak Base Ion Exchanger

Haslaniza Hashim , Saiful Irwan Zubairi , Wan Aida Wan Mustapha, and Mohamad Yusof Maskat 

School of Chemical Sciences & Food Technology, Faculty of Science & Technology, Universiti Kebangsaan Malaysia (UKM), 43600 Bangi, Selangor, Malaysia

Correspondence should be addressed to Haslaniza Hashim; [haslaniza@ukm.edu.my](mailto:haslaniza@ukm.edu.my)

Received 1 February 2018; Accepted 19 April 2018; Published 5 June 2018

Academic Editor: Branca Silva

Copyright © 2018 Haslaniza Hashim et al. This is an open access article distributed under the Creative Commons Attribution License, which permits unrestricted use, distribution, and reproduction in any medium, provided the original work is properly cited.

Although noni (*Morinda citrifolia* L.) has been used to treat a broad range of diseases, many people avoid consuming the fruits because of its unpleasant odor caused by organic acids. Even though ion exchange resins were able to reduce the odor, it also reduced beneficial antioxidant compounds. Thus, to preserve antioxidants (phenolic compounds) during deacidification, it is important to characterize the interaction of ion exchange resin with both organic acids and phenolic compounds. Adsorption capacities of organic acids and phenolic compounds commonly found in the noni fruit were conducted onto Amberlite IRA 67 resin. The phase contact time to reach equilibrium for octanoic acid and hexanoic acid compounds was 326.86 and 160.72 min, respectively. The values of initial adsorption rate,  $1/K_1$ , and adsorption extent,  $1/K_2$ , decreased with the increase of initial concentration for all compounds studied. Results for all the compounds studied fitted well to the Langmuir model. The effect of pH in adsorption capacity of the actual system (noni juice) has been applied based on the model system studied.

## 1. Introduction

*Morinda citrifolia* L. or noni is one of the traditional folk medicinal plants that has been used for over 2000 years in Polynesia. According to the European Commission [1], it has been accepted in the European Union as a novel food. However, noni extracts exude a strong unpleasant odor. The unpleasant odor of noni extract, contributed by medium-chain fatty acids such as caproic (hexanoic) and caprylic (octanoic) acid [2], decreases the level of consumers' acceptance.

Deacidification is a process that is used to reduce the level of acid in food systems. Ion exchange and adsorbent resins have shown promising results in the modification of acids in fruit juice. Several studies to deacidify fruit juices using ion exchange resin have also been performed on passion fruit [3]. However, although the unpleasant odor was reduced, antioxidant activities were also reduced.

Haslaniza et al. [4] reported that noni juice treated with weak base anion exchange resin (Amberlite IRA 67) showed promising potential in reduction of octanoic and hexanoic acids while it also gave minimal reduction on antioxidant content. Increased attention has been given on the role of natural antioxidants, in particular, phenolic compounds, which may act both by reducing the content of toxic compounds in foods and by supplying the human body with exogenous antioxidants [5]. Due to the beneficial role of antioxidants, it is important that deacidification did not reduce the antioxidant activity in the noni juice.

To characterize the adsorption process, Peleg's model can be used to determine the equilibrium phase contact time and maximum adsorption yield throughout the process. As reported by previous researchers, the model has been used to describe sorption processes in various food systems [6–8]. Poojary and Passamonti [9] also applied this model to

predict the kinetics and modelling in the extraction of lycopene in tomato waste using organic solvents. Peleg's model adequately describes the rate of the adsorption process, adsorption extent, and exhaustive time of the compounds studied. Meanwhile, the Langmuir and Freundlich models can be used to predict the adsorption isotherm for the compounds studied.

In order to reduce the unpleasant odor of noni juice but at the same time conserve the antioxidants during the deacidification process, it is important to understand the interaction of both unpleasant odor compounds of organic acids and antioxidants with ion exchange resins. Thus, this study was carried out to determine the adsorption characteristics between organic acids (octanoic acid and hexanoic acid) and phenolic compounds (rutin, scopoletin, and quercetin) onto a weakly basic ion exchange resin using a model system.

## 2. Materials and Methods

**2.1. Materials.** Weak base anion exchanger Amberlite IRA 67 and standards of octanoic acid, hexanoic acid, rutin, scopoletin, and quercetin were purchased from Sigma-Aldrich Corporation (St. Louis, MO, USA). Amberlite IRA 67 was used due to its higher performance for the adsorption of some organic acid compounds as reported by Haslaniza et al. [4]. Rutin, scopoletin, and quercetin were used due to its existence in all noni fruits and commercial noni juices from different countries all over the world although at different ranges of concentration [10]. Methanol (HPLC grade, purity >99.9%) was purchased from Fisher Scientific (New Jersey, USA).

**2.2. Adsorption Studies of Organic Acids and Phenolic Compounds.** The adsorption studies of organic acids and phenolic compounds onto weakly basic ion exchanger resin were carried out in Erlenmeyer flasks where 0.1 g of the dry anion exchanger and 0.02 L of each sample which were octanoic acid (250, 500, 750, and 1000 mg/L), hexanoic acid (100, 200, 300, and 400 mg/L), rutin (25, 50, 75, and 100 mg/L), scopoletin (25, 50, 75, and 100 mg/L), and quercetin (25, 50, 75, and 100 mg/L) were added without pH adjustment. The flasks were agitated in an orbital shaker (WiseCube, Daihan Scientific, Korea) at a constant speed of 120 rpm for 180 min at room temperature (25°C) to achieve equilibrium [11]. Each of the organic acid after equilibrium was measured using a gas chromatographer (Agilent, Model HP6890, USA) equipped with a flame ion detector (FID). Each of the phenolic compounds was measured using high-performance liquid chromatography (HPLC). The amount of organic acids and phenolic compounds adsorbed at equilibrium,  $q_e$  (mg/g), were calculated using the following equation:

$$q_e = \frac{C_o - C_e}{w} \times V, \quad (1)$$

where  $C_o$  and  $C_e$  were the concentrations (mg/L) of each organic acid and phenolic compound at the beginning

and after equilibrium, respectively,  $V$  was the volume of the solution (L), and  $w$  was the mass of the dry anion exchanger (g).

**2.3. Kinetics of Liquid-Liquid Adsorption.** The Peleg model has been used to describe adsorption processes in various foods [12–14]. The adsorption curves (concentration of each organic acid/phenolic compound versus time) could be described by a model proposed by Peleg [15] which in case of adsorption would assume the form as stated below:

$$C(t) = C_o + \frac{t}{K_1 + K_2 \cdot t}, \quad (2)$$

where  $C(t)$  is the concentration of each organic acid/phenolic compound at time  $t$  (mg/g),  $t$  is the adsorption time (min),  $C_o$  is the initial concentration of each organic acid/phenolic compound at time  $t = 0$  (mg/g),  $K_1$  is Peleg's rate constant (min·g/mg), and  $K_2$  is Peleg's capacity constant (g/mg). Equation (2) was used in the final form while  $C_o = 0$  in all experiments:

$$C(t) = \frac{t}{K_1 + K_2 \cdot t}. \quad (3)$$

$K_1$  is Peleg's rate constant which is related to adsorption rate ( $B_0$ ) at the very beginning ( $t = t_0$ ):

$$B_0 = \frac{1}{K_1} \left( \frac{\text{mg}}{\text{g}} \cdot \text{min} \right). \quad (4)$$

$K_2$  is Peleg's capacity constant which is related to maximum adsorption yield or equilibrium concentration of adsorbed compounds ( $C_e$ ). When  $t \rightarrow \infty$ ,

$$C(t \rightarrow \infty) = C_e = \frac{1}{K_2} \left( \frac{\text{mg}}{\text{g}} \right). \quad (5)$$

**2.4. Determination of Organic Acids.** Organic acids (octanoic acid and hexanoic acid) were extracted using Gas Chromatography Solid Phase Microextraction (GC-SPME). The SPME inlet used was 0.75 mm (Supelco). SPME needle contained divinylbenzene-carboxen-polydimethylsiloxane (DVB-CAR-PDMS) fiber (StableFlex, Supelco). The sample (1 mL) was added into a headspace vial, sealed with silicone septum, and layered with Teflon-faced silicone septa (Supelco, USA). Then, it was heated in a waterbath (Memmert, Germany) at 53°C for 12 min [16]. After heating, SPME needle was directly injected through the septum into the vial for 10 min. After extraction, the needle was removed from the vial and injected to the gas chromatographer.

Gas chromatography was performed using a gas chromatographer mass spectrometry (Agilent, Model HP6890, USA) equipped with a flame ion detector (FID) and splitless injector. Separation of the organic compounds was done using a capillary column HP-5 (30 m × 0.25 i.d., 0.25 μm film thickness, J&W Scientific Pte Ltd., USA). Oven temperature was programmed according to the method of Zambonin et al. [17] with the following parameters: initial temperature was 50°C for 2 min before it raised to 80°C at 20°C/min for

1 min and then heated to 100°C at 20°C/min for 1 min. When it reached 100°C, the temperature finally rose to 250°C at 30°C/min and was held for 2 min. The gas flow rate was maintained at 40 cm<sup>3</sup>/s with nitrogen (N<sub>2</sub>) used as carrier gas. The total separation time for each samples were 13.5 min. Volatile compounds were identified by comparing the peak retention time to those of pure standard with the peak retention time for deacidified samples. The analysis was expressed as concentration (mg/L) obtained from the software.

**2.5. Determination of Phenolic Compounds.** Determination of phenolic compounds was carried out using high-performance liquid chromatography (HPLC) as reported by Haslaniza et al. [4]. The standards (scopoletin, rutin, and quercetin) were weighed and dissolved in appropriate volume of methanolic solution using deionized water to produce stock standard solutions. To construct calibration curves for each standard, the working standard was prepared by diluting stock standard solutions with methanolic solution at different concentrations. Before injected into HPLC instrumentation, samples were filtered through a 0.22 μm membrane filter (Iwaki Glass).

The determination of selected phenolic compounds was determined by the modified Analytical HPLC Application 031481, Merck, USA (2008) method for an HPLC system. Briefly, the samples/standard solutions (20 μL) were injected into a Shimadzu chromatographer 20A coupled with photodiode array detector (PDA), equipped with Chromolith Performance RP-18 endcapped, Merck, UK (Cat. number 1.02129). The pump was connected to two mobile phases: A, methanol/deionized water (2.5 : 97.5, v/v) and B, methanol/deionized water (50 : 50, v/v). The elution flow rate was 2.1 mL/min at 25 min with a column temperature maintained at 30°C. The mobile phase was set as a linear gradient as it afforded a good separation and symmetrical peak shape of target analytes in the chromatograms. Then, it was programmed as follows: 0–10 min, 100% A, 0% B; 10–15 min, 65% A, 35% B; 15–20 min, 0% A, 100% B; 20–22 min, 100% A, 0% B; and 22–25 min, 100% A, 0% B. The PDA spectra was monitored in the range of 210 to 450 nm and quantified at 365 nm. Data analyses were done using Shimadzu Lab Solution software.

**2.6. Adsorption Isotherm.** The adsorption isotherm indicated how the adsorption molecules distribute between the liquid phase and the solid phase when the equilibrium state was reached [18]. The data of the adsorption process for the organic acids and three phenolic compounds were analyzed using the Langmuir isotherm linear model according to the following equation [19]:

$$\frac{C_e}{q_e} = \frac{1}{q_m} C_e + \frac{1}{K_L q_m}, \quad (6)$$

where  $q_e$  is the adsorption capacity of each compound at equilibrium (mg/g),  $C_e$  is the equilibrium concentration of each compound (mg/L),  $K_L$  is a Langmuir adsorption constant which is related to the affinity of the adsorption

(L/mg), and  $q_m$  is a maximum capacity or the amount of organic acids adsorbed at complete monolayer coverage (mg/g). The values of  $K_L$  and  $q_m$  are obtained from the intercept and slope, respectively, of the straight line plot of  $C_e/q_e$  versus  $C_e$ . Another model Freundlich adsorption isotherm and its linearized form are given in the following equations [18]:

$$q_e = K_F + C_e^{1/n}, \quad (7)$$

$$\log q_e = \log K_F + \frac{1}{n} \log C_e, \quad (8)$$

where  $K_F$  and  $1/n$  are the Freundlich equilibrium coefficients related to the adsorption capacity and adsorption intensity, respectively [20]. A plot of  $\log q_e$  versus  $\log C_e$  gives a straight line with a slope ( $1/n$ ) and an intercept at  $\log K_F$ .

The favorability of the sorption system in the batch process was estimated from the shape of the isotherm which may be indicated by essential characteristics of the Langmuir isotherm, expressed in terms of a dimensionless constant separation factor  $R_L$ , given by the following equation [21]:

$$R_L = \frac{1}{1 + K_L C_o}, \quad (9)$$

where  $K_L$  is the Langmuir constant (L/mg) and  $C_o$  is the initial organic acid concentration (mg/L). The value of  $R_L$  indicates whether the isotherm is unfavourable ( $R_L > 1$ ), linear ( $R_L = 1$ ), favourable ( $0 < R_L < 1$ ), or irreversible ( $R_L = 0$ ) [22, 23].

**2.7. Statistical Methods.** Data were analyzed using Statistical Analytical System (SAS) version 9.1.3 for  $T$ -test. All experiments were done using three replications. The parameters of modified Peleg's model (constants  $K_1$  and  $K_2$ ) were determined from experimental data. Validation between the experimental data and predicted value was established by root mean squared deviation (RMSD) as described by Pineiro et al. [24] using the following equation:

$$\text{RMSD} = \sqrt{\frac{1}{n} \sum (\text{experimental} - \text{predicted})^2}. \quad (10)$$

### 3. Results and Discussion

**3.1. Adsorption Capacity and Exhaustive Time Characteristics as Influenced by Initial Concentration.** The influence of different concentrations of octanoic and hexanoic acids on adsorption capacity at 303 K and 120 rpm agitation speed can be seen in Figure 1. The concentrations of adsorbed compounds were calculated according to (1). The adsorption curves indicate the exponential adsorption rate for all concentration ranges studied.

From Figure 1, the plot reveals rapid uptake at the initial stages, followed by a gradual increase as equilibrium was reached. The adsorption capacity was higher initially due to greater availability of vacant sites for adsorption. After a period of time, the number of vacant sites became less, and eventually, all available sites became saturated [25]. As

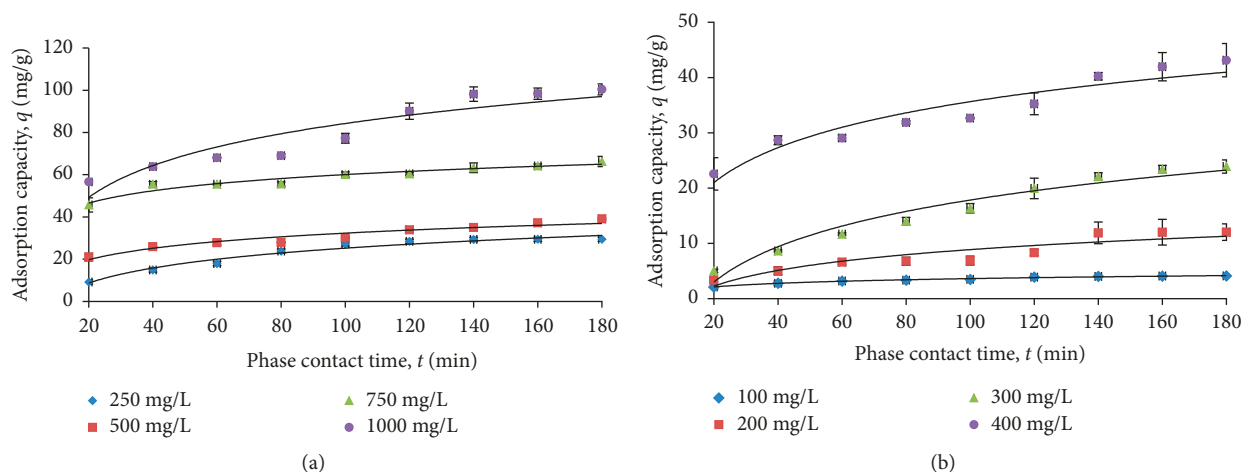


FIGURE 1: Kinetic of (a) octanoic acid and (b) hexanoic acid adsorption onto a weak base ion exchange resin (Amberlite IRA 67) at different organic acid concentrations. Graph represents the mean of three replicate samples with error bars.

TABLE 1: Values of adsorption extent, Peleg's constants ( $K_1$  and  $K_2$ ) for adsorption of octanoic acid with regression coefficient ( $R^2$ ), and the root mean squared deviation (RMSD) at different initial concentrations.

Initial concentration (mg/L)	Adsorption extent (mg/g)	$K_1$ (min·g/mg)	$K_2$ (g/mg)	$R^2$	RMSD (adsorption extent)	Exhaustive time (Peleg)	RMSD (exhaustive time)
250	$37.04 \pm 2.26$	$1.086 \pm 0.082$	$0.027 \pm 0.004$	0.920	0.79	$313.09 \pm 4.17$	5.51
500	$41.67 \pm 2.20$	$0.497 \pm 0.025$	$0.024 \pm 0.000$	0.966	0.63	$326.01 \pm 4.12$	4.65
750	$71.43 \pm 3.46$	$0.132 \pm 0.068$	$0.014 \pm 0.005$	0.993	0.16	$330.85 \pm 3.53$	2.33
1000	$111.11 \pm 4.69$	$0.196 \pm 0.041$	$0.009 \pm 0.001$	0.942	0.77	$337.47 \pm 4.80$	2.66

TABLE 2: Values of adsorption extent, Peleg's constants ( $K_1$  and  $K_2$ ) for adsorption of hexanoic acid with regression coefficient ( $R^2$ ), and the root mean squared deviation (RMSD) at different initial concentrations.

Initial concentration (mg/L)	Adsorption extent (mg/g)	$K_1$ (min·g/mg)	$K_2$ (g/mg)	$R^2$	RMSD (adsorption extent)	Exhaustive time (Peleg)	RMSD (exhaustive time)
100	$4.44 \pm 0.23$	$4.07 \pm 0.60$	$0.225 \pm 0.015$	0.98	0.01	$155.44 \pm 4.75$	1.68
200	$14.93 \pm 1.10$	$4.28 \pm 0.35$	$0.067 \pm 0.012$	0.75	0.02	$159.85 \pm 4.12$	0.53
300	$33.33 \pm 1.79$	$2.52 \pm 0.14$	$0.030 \pm 0.000$	0.75	0.43	$162.72 \pm 3.47$	0.39
400	$45.45 \pm 0.54$	$0.49 \pm 0.17$	$0.022 \pm 0.000$	0.96	0.67	$164.86 \pm 4.23$	0.34

mentioned by Amin [26] and Kannan and Sundaram [27], the rate of organic acids removal was controlled by the rate of organic acids transported to the exterior sites of the adsorbent until all available surface sites were fully occupied after the initial adsorption. As other variables such as resin mass, temperature, and agitation speed were the same for different experimental runs, the organic acids concentration affected the diffusion of organic acids molecules through the solution to the surface of the Amberlite IRA 67. Higher concentration resulted in a higher driving force of the concentration gradient [22]. This driving force accelerated the diffusion of organic acids from the solution onto the adsorbent [28]. This phenomenon of adsorption is well described by Peleg's model [15]. The experimental adsorption extent, calculated parameters of modified Peleg's model (constants  $K_1$  and  $K_2$ ), regression coefficient ( $R^2$ ), and RMSD are shown in Tables 1 and 2. The  $R^2$  was high for both octanoic and hexanoic acids ( $R^2 > 0.75$ ) with the  $p$  values less than 0.05 which showed adequate presentation of the experimental and data by Peleg's model.

The initial adsorption rate and the maximum adsorption extent in experimental conditions were calculated from constant  $K_1$  and  $K_2$  using (4) and (5).  $K_1$  decreased as initial concentrations of both octanoic acid and hexanoic acid increased indicating increased adsorption rates with increasing initial concentration of octanoic acid and hexanoic acid.  $K_2$  is a constant inversely related to maximum adsorption capacity. When  $K_2$  is lower, the adsorption capacity is higher [12].  $K_2$  for octanoic acid and hexanoic acid decreased linearly with increasing concentration as presented in Tables 1 and 2. When the octanoic acid and hexanoic acid concentrations did not vary with the phase contact time, the adsorption equilibrium is accomplished. According to data obtained from the Peleg model extrapolation (data not shown), equilibrium time was found to be 326.86 min for octanoic acid and 160.72 min for hexanoic acid which were statistically different ( $p < 0.05$ ).

Figure 2 displays the influence of different concentrations of rutin, scopoletin, and quercetin on adsorption capacity at 303 K and 120 rpm agitation speed. The three

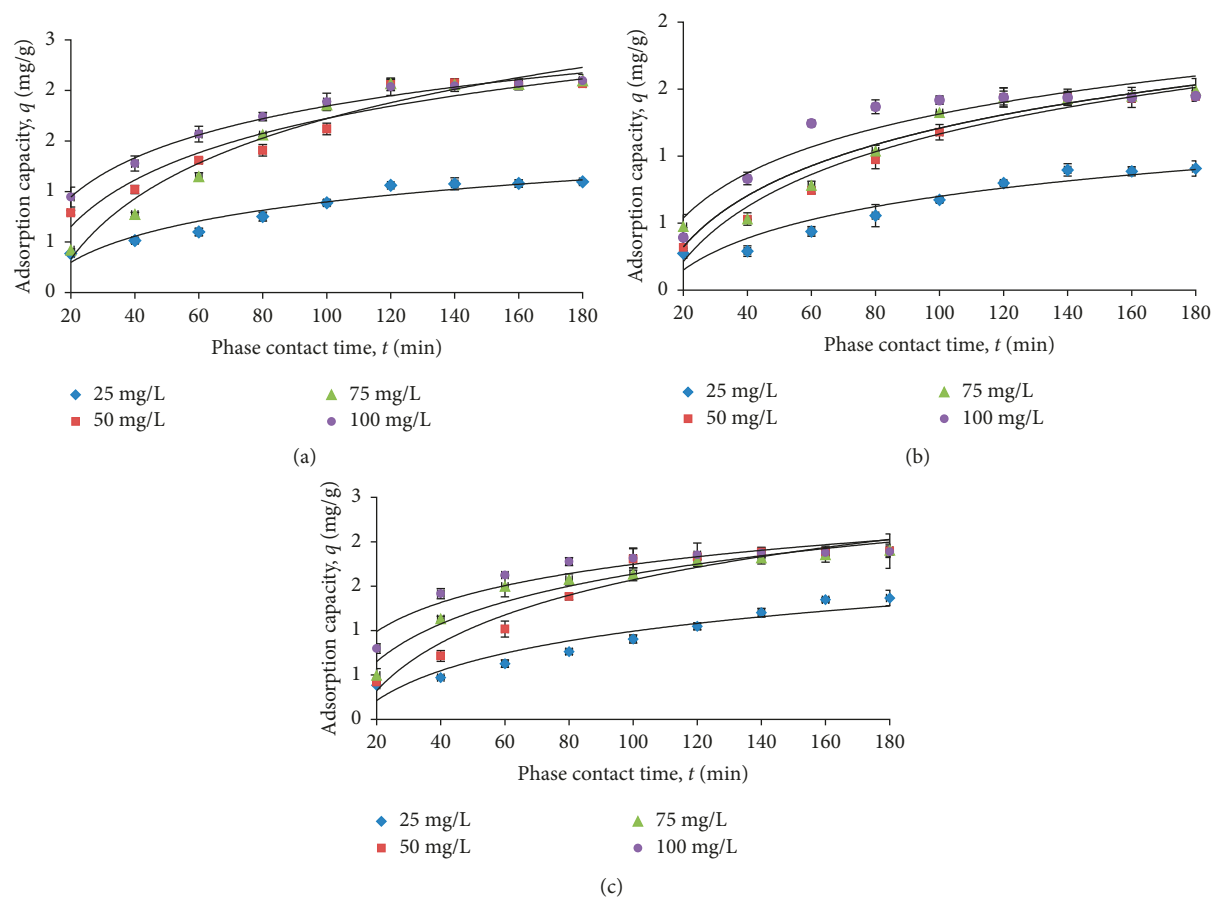


FIGURE 2: Kinetic of (a) rutin, (b) scopoletin, and (c) quercetin adsorption onto a weak-base ion exchange resin (Amberlite IRA 67) at different phenolic compound concentrations. Graph represents the mean of three replicate samples with error bars.

curves show the exponential increase of adsorption rate for each individual antioxidant at given contact time (180 min) for four different initial concentrations from 25 to 100 mg/L. As can be seen in Figure 2, the three curves gave similar adsorption profiles. Similar to organic acids, the adsorption capacities of phenolic compounds increased as time increased due to the higher amount of phenolic compounds adsorbed onto the weakly basic anion exchanger. After a certain period of time, the adsorption rate decreased as it reached the equilibrium point. The equilibrium point was reached when all of the antioxidant compounds adsorbed to the resin (at lower antioxidant concentration) or the vacant sites of Amberlite IRA 67 were fully occupied (at higher antioxidant concentration). The decreased adsorption rate after equilibrium might happen due to the physical adsorption (physisorption) of the phenolic compounds and Amberlite IRA 67. In physical adsorption, the weak van der Waals forces act. It involves the weak force attraction between the adsorbate and adsorbent, and therefore, this type of adsorption can be easily reversed. Similar phenomenon happened in this study where the phenolic compounds are not fixed to the Amberlite IRA 67 and can move freely within the interfacial surfaces [29].

According to Peleg's value for the individual antioxidant compounds as shown in Tables 3–5,  $K_1$  values

decreased suggesting a corresponding increase in the initial adsorption rates of the phenolic compounds with increasing concentration. Zin et al. [5] and Hasnain et al. [22] reported that most phenolic compounds found in the noni fruit are nonpolar in nature including the phenolic compounds studied. High porosity and hydrophobic nature of resins has been reported to allow the adsorption of non-polar phenolic compounds through hydrophobic interactions [30] and van der Waals forces [31]. Thus, it is highly probable that, different from organic acids, adsorption of antioxidant compounds from noni juice is also due to the hydrophobic interaction. The  $K_2$  values for rutin, scopoletin, and quercetin also decreased as concentration increased. The adsorption extent was influenced by the initial concentration of phenolic compounds.  $R^2$  for these three phenolic compounds were acceptable ( $R^2 > 0.75$ ). The RMSD had relatively a low value for the compounds.

Increasing adsorption rate, namely, decreasing  $K_1$ , with increasing initial concentration is expected adsorption behaviour. The same phenomenon happened in water absorption in chickpea during soaking [12]. Table 6 shows fitting of Peleg's rate constant and  $K_1$  for organic acids and phenolic compounds at different initial concentrations. As discussed earlier,  $K_1$  decreased as initial concentration of organic acids and antioxidants increased. As summarized in

TABLE 3: Values of adsorption extent, Peleg's constants ( $K_1$  and  $K_2$ ) for adsorption of rutin with regression coefficient ( $R^2$ ), and the root mean squared deviation (RMSD) at different initial concentrations.

Initial concentration (mg/L)	Adsorption extent (mg/g)	$K_1$ (min·g/mg)	$K_2$ (g/mg)	$R^2$	RMSD (adsorption extent)	Exhaustive time (Peleg)	RMSD (exhaustive time)
25	1.34 ± 0.08	33.43 ± 0.82	0.75 ± 0.029	0.89	0.01	335.69 ± 5.52	0.18
50	2.47 ± 0.03	15.55 ± 0.84	0.41 ± 0.006	0.91	0.01	345.15 ± 4.83	1.15
75	3.05 ± 0.12	25.06 ± 0.53	0.33 ± 0.006	0.75	0.10	341.65 ± 6.59	2.76
100	2.33 ± 0.26	9.28 ± 0.31	0.43 ± 0.043	0.98	0.05	67.88 ± 2.80	3.14

TABLE 4: Values of adsorption extent, Peleg's constants ( $K_1$  and  $K_2$ ) for adsorption of scopoletin with regression coefficient ( $R^2$ ), and the root mean squared deviation (RMSD) at different initial concentrations.

Initial concentration (mg/L)	Adsorption extent (mg/g)	$K_1$ (min·g/mg)	$K_2$ (g/mg)	$R^2$	RMSD (adsorption extent)	Exhaustive time (Peleg)	RMSD (exhaustive time)
25	1.19 ± 0.119	61.47 ± 1.06	0.84 ± 0.043	0.75	0.02	465.51 ± 7.89	0.68
50	2.02 ± 0.15	38.37 ± 2.39	0.50 ± 0.018	0.76	0.01	466.76 ± 8.47	1.20
75	1.88 ± 0.09	30.64 ± 0.53	0.53 ± 0.015	0.82	0.03	392.14 ± 9.07	1.17
100	1.68 ± 0.04	17.80 ± 2.02	0.60 ± 0.012	0.92	0.02	21.78 ± 1.66	0.48

TABLE 5: Values of adsorption extent, Peleg's constants ( $K_1$  and  $K_2$ ) for adsorption of quercetin with regression coefficient ( $R^2$ ), and the root mean squared deviation (RMSD) at different initial concentrations.

Initial concentration (mg/L)	Adsorption extent (mg/g)	$K_1$ (min·g/mg)	$K_2$ (g/mg)	$R^2$	RMSD (adsorption extent)	Exhaustive time (Peleg)	RMSD (exhaustive time)
25	1.76 ± 0.11	41.81 ± 2.31	0.57 ± 0.017	0.76	0.00	214.07 ± 3.15	0.28
50	2.24 ± 0.08	15.06 ± 0.88	0.45 ± 0.007	0.93	0.00	216.23 ± 4.18	1.51
75	1.70 ± 0.81	26.15 ± 1.09	0.37 ± 0.066	0.77	0.08	214.63 ± 4.82	1.71
100	2.06 ± 0.22	7.27 ± 0.64	0.49 ± 0.038	0.98	0.06	203.52 ± 6.41	3.84

Table 6, octanoic acid, hexanoic acid, and scopoletin fitted the linear regression model while rutin and quercetin fitted the nonlinear regression model. It can be clearly observed that the rate of adsorption with increasing concentration for the antioxidant compounds were higher compared to the organic acids. This further explained the reduction of antioxidant activity during deacidification.

$K_2$  is a constant related to adsorption capacity. The lower the  $K_2$ , the higher the adsorption capacity [12]. Table 8 shows fitting of Peleg's capacity constant and  $K_2$  for organic acids and phenolic compounds at different initial concentrations. According to Table 7, octanoic acid, hexanoic acid, and scopoletin fitted the linear regression model while rutin and quercetin fitted the nonlinear regression model similar to the trend in  $K_1$ . However, based on the  $R^2$  value, data for scopoletin were not adequately represented by the model. The  $p$  values for scopoletin also were slightly higher than 0.05 indicated that the compound was not significant. Similar to  $K_1$ , rate of increase for  $K_2$  of rutin and quercetin was higher than octanoic and hexanoic acids.

**3.2. Equilibrium Isotherm.** The Langmuir isotherm model has been used to describe the adsorption isotherm of compounds studied (organic acids and phenolic compounds) which involved the relation between adsorption capacity and solution concentration as mentioned by Parsaei and Goodarzi [32]. The adsorption isotherm indicated how the adsorption molecules distribute between the liquid phase and the solid phase when the equilibrium

TABLE 6: Equation and regression coefficient of Peleg's rate constant for organic acids (octanoic acid and hexanoic acid) and phenolic compounds (scopoletin, quercetin, and rutin) at different initial concentrations.

Compound	Equation	Regression coefficient, $R^2$
Octanoic acid	$y = -0.001x + 1.236$	0.809
Hexanoic acid	$y = -0.012x + 5.965$	0.848
Rutin	$y = -13.8 \ln(x) + 76.44$	0.616
Scopoletin	$y = -0.555x + 71.75$	0.953
Quercetin	$y = -20.7 \ln(x) + 105.8$	0.692

TABLE 7: Equation and regression coefficient of Peleg's capacity constant for organic acids (octanoic acid and hexanoic acid) and phenolic compounds (scopoletin, quercetin, and rutin) at different initial concentrations.

Compound	Equation	Regression coefficient, $R^2$
Octanoic acid	$y = -3E - 05x + 0.034$	0.961
Hexanoic acid	$y = -0.000x + 0.247$	0.775
Rutin	$y = -0.26 \ln(x) + 1.526$	0.716
Scopoletin	$y = -0.18x + 1.364$	0.527
Quercetin	$y = -0.08 \ln(x) + 0.825$	0.408

state was reached [18]. The Langmuir isotherm model assumes that intermolecular forces between adsorbing molecules are negligible and that once available sites on adsorbent are fully occupied, no further adsorption takes place [25]. Meanwhile, the Freundlich isotherm describes

TABLE 8: Langmuir and Freundlich isotherm constants and correlation coefficients for octanoic acid adsorption by Amberlite IRA 67.

Compound	Langmuir isotherm coefficients				Freundlich isotherm coefficients			
	Equation	$q_m$ (mg/g)	$K_L$ (L/mg)	$R^2$	Equation	$n$ (mg/g)	$K_F$ (L/mg)	$R^2$
Octanoic acid	$y = -0.004x + 7.34$	250.00	$5.45 \times 10^{-4}$	0.86	$y = 1.213x - 1.286$	0.8244	0.28	0.99
Hexanoic acid	$y = -0.139x + 26.65$	7.19	$5.22 \times 10^{-3}$	0.78	$y = 2.890x - 4.805$	0.346	0.0082	0.92
Rutin	$y = 0.371x - 0.583$	2.70	0.6364	0.81	$y = 0.308x - 0.057$	3.247	1.059	0.28
Scopoletin	$y = -0.556x - 4.207$	1.80	0.1322	0.94	$y = 0.013x + 0.318$	76.92	1.374	0.00
Quercetin	$y = -0.451x - 2.849$	2.22	0.1583	0.94	$y = -0.022x + 0.456$	45.45	1.578	0.02

heterogeneous systems and reversible adsorption, and is not limited to the formation of a complete monolayer [22].

**3.3. Organic Acids.** For organic acids (octanoic and hexanoic acids), the adsorption data were applied to both linearized form of Langmuir and Freundlich equations. According to Table 8, for octanoic acid, the values of  $R^2$ , 0.86 for Langmuir and 0.99 for Freundlich, suggest that both homogeneous and heterogeneous monolayer mechanism in the adsorption process were at play. The values of the Langmuir dimensionless separation factor  $R_L$  lie between 0 and 1 (Table 9). Hence, the sorption system may be considered favourable by the Langmuir model. Similar to the  $R_L$  value from the Langmuir isotherm, the  $n$  value from the Freundlich isotherm is related to the adsorption intensity where  $n > 1$  indicates good adsorption over different equilibrium concentrations [33, 34]. If  $n$  value  $< 1$ , adsorption intensity is only good at high concentration [34]. As shown in Table 8, the  $n$  value found to be 0.8244 for octanoic acid adsorption by Amberlite IRA 67 suggested that it is more suitable at high concentration only. The maximum monolayer capacities  $q_m$  for sorption of octanoic acid were 250.00 mg/g.

Table 8 also shows the Langmuir and Freundlich isotherm models of hexanoic acid sorption on Amberlite IRA 67. The values of  $R^2$  were found to be 0.78 for Langmuir and 0.92 for Freundlich. The value of the Langmuir dimensionless separation factor  $R_L$  for hexanoic acid was between 0 and 1, indicating that the sorption process is favourable for this adsorbent [25]. The  $n$  value of 0.346 from the Freundlich isotherm also indicates that hexanoic acid adsorption which is only suitable at high concentration. The maximum monolayer capacities  $q_m$  for sorption of hexanoic acid were 7.19 mg/g. For both organic acids studied, the observed data (Table 9) show that  $R_L$  values decrease with increasing concentration suggesting that the organic acids uptake process is more favourable with higher concentration of organic acids as reported by [35] in the biosorption of metal dyes onto *Agave americana* (L) fibres.

**3.4. Phenolic Compounds.** The data of adsorption process for the three phenolic compounds (rutin, scopoletin, and quercetin) were analyzed using the Langmuir isotherm linear model. The linearized form of the Langmuir isotherm of each phenolic compound on Amberlite IRA 67 resin was found to be linear over the whole concentration range studied, and the correlation coefficients were high ( $> 0.8$ ) while the correlation coefficients for the Freundlich isotherm were low ( $< 0.3$ ). The high degree of correlation for the

TABLE 9:  $R_L$  values for Amberlite IRA 67 on the adsorption of organic acids and phenolic compounds.

Compound	Initial concentration $C_o$ (mg/L)	$R_L$
Octanoic acid	250	0.7672
	500	0.6223
	750	0.5234
	1000	0.4517
Hexanoic acid	100	0.7074
	200	0.5472
	300	0.4462
	400	0.3767
Rutin	25	0.0642
	50	0.0332
	75	0.0224
	100	0.0169
Scopoletin	25	0.0094
	50	0.0070
	75	0.0047
	100	0.0035
Quercetin	25	0.01385
	50	0.00697
	75	0.00466
	100	0.00350

linearized Langmuir relationship suggested that a single surface reaction with constant activation energy was the predominant rate-controlling step [36].

As observed in Table 8, the results shows that the adsorption capacity ( $q_m$ ) of rutin, scopoletin, and quercetin was found to be 2.70, 1.80, and 2.22 mg/g, respectively, using the linearized Langmuir isotherm model. The adsorption mechanism seems to obey the homogeneous monolayer model better than the heterogeneous model. The favorability of the adsorption process for the phenolic compounds is reflected by the Langmuir dimensionless separation factor ( $0 < R_L < 1$ ) [25] as shown in Table 9. Similar to organic acids, the  $R_L$  values decrease with increasing initial concentration suggesting that the phenolic compounds uptake process is more favourable at higher concentration. The good correlation coefficients and the values of  $R_L$  confirmed that the Langmuir isotherm is a suitable isotherm for adsorption of each phenolic compound onto Amberlite IRA 67 resin compared to the Freundlich isotherm.

Adsorption capacity ( $q_m$ ) of all phenolic compounds was lower than both organic acids showing lower adsorption capacities. However, all three phenolic compounds showed higher  $K_L$  values than both organic acids. This suggest that the phenolic compounds have higher adsorption affinity towards organic acids which may contribute to the higher

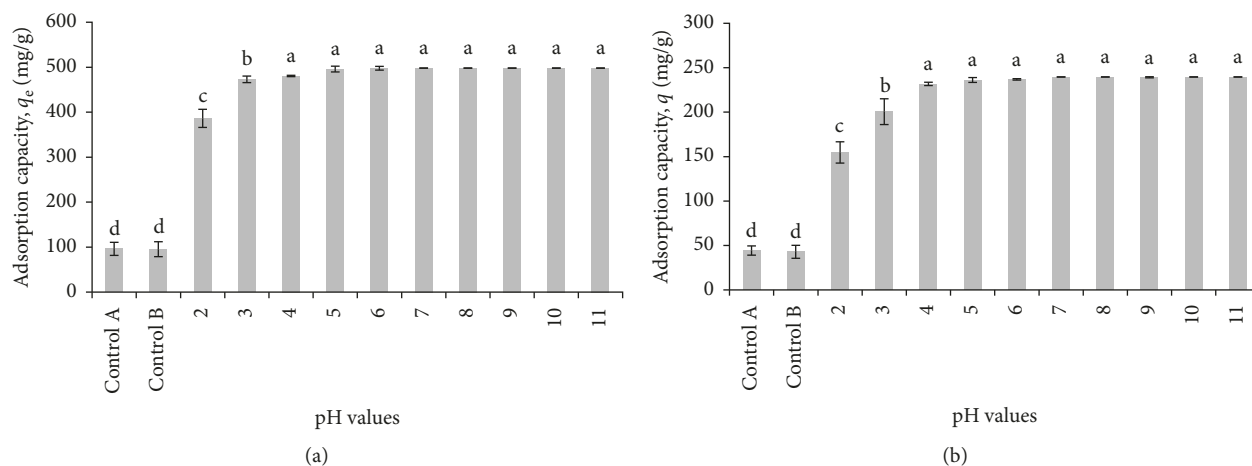


FIGURE 3: Effect of pH of (a) octanoic acid and (b) hexanoic acid adsorption in noni juice onto a weak base ion exchange resin (Amberlite IRA 67) at different pH. Graph represents the mean of three replicate samples with error bar. Different letters on the bars indicate significant differences ( $p < 0.05$ ).

rate of Peleg's  $K_1$  constant as shown in Table 6. The results indicate that, in its present characteristics, it would be difficult to reduce the adsorption of phenolic compounds.

**3.5. Actual System.** pH plays an important role in the adsorption process, particularly on the adsorption capacity [22]. In order to determine the actual interaction of studied compounds, the influence of pH on adsorption of organic acids (octanoic and hexanoic acid) and phenolic compounds (rutin, scopoletin, and quercetin) has been applied in noni juice based on the model system.

The effect of pH in the solution on the adsorption capacity,  $q_e$  (mg/g), of organic acids in noni juice on Amberlite IRA 67 was studied at a pH range of 2–11 as shown in Figure 3. The experiment was performed with initial octanoic and hexanoic acid concentrations of 249.03 and 104.21 mg/L, respectively, at 303 K with a contact time of 327 min. As can be seen in Figure 3, there was a similar trend in adsorption capacity of both organic acids onto weak base ion exchange resin Amberlite IRA 67. Control samples A (noni juice without resin and agitation) and B (noni juice without resin with agitation) show no significant difference for both organic acids. Agitation rate and time did not influence much to the concentration of organic acids. However, adsorption capacity of organic acids in noni juice is significantly ( $p < 0.05$ ) increased when treated at different pH compared to control samples. For both organic acids, noni juice treated at pH 2 showed the lowest ( $p < 0.05$ ) adsorption capacity. As the pH increased, adsorption capacity also increases up to pH 5. No significant difference was observed between samples of pH 5 to 11. It explained that the maximum removal of organic acids (octanoic and hexanoic acid) by Amberlite IRA 67 was achieved at pH 4.

From the observation, adsorption capacity of organic acids increases with increasing pH values. It might be due to the rate of protonation of the compounds in aqueous solution. As reported by Berbar et al. [37], during the adsorption of

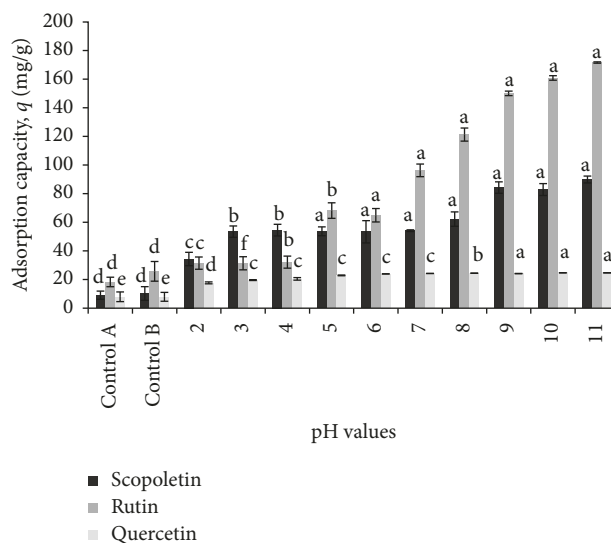


FIGURE 4: Effect of pH of phenolic compounds (scopoletin, rutin, and quercetin) adsorption in noni juice onto a weak base ion exchange resin (Amberlite IRA 67) at different pH. Graph represents the mean of three replicate samples with error bars. \*Different letters in the same phenolic compounds indicate significant difference ( $p < 0.05$ ).

polyethyleneimine using anion exchange resin, adsorption is more favoured at low acidic solution but not at strong acidic condition. It happened due to the reduction of the positive repulsive interactions between functional groups at high pH. This explained the effect of pH of solution on the adsorption of organic acids (octanoic and hexanoic acids) onto resin surface.

Figure 4 indicates the effect of pH on the adsorption capacity,  $q_e$  (mg/g), of phenolic compounds (scopoletin, rutin, and quercetin) in noni juice using Amberlite IRA 67 at a pH range of 2–11. The experiment was conducted with initial scopoletin, rutin, and quercetin concentration of 52.34, 86.23, and 12.46 mg/L, respectively, at 303 K with a contact

time of 327 min. As expected, no significant difference was observed in control samples A (noni juice without resin and agitation) and B (noni juice without resin and with agitation). It means that agitation time and rate also did not affect both the control samples. According to Figure 4, adsorption capacity of these three phenolic compounds in noni juice was low at highly acidic medium and gradually increased with increasing pH values up to pH 11, except quercetin. The highest ( $p < 0.05$ ) adsorption capacity of scopoletin was found at pH 5 and remained constant until pH 11, whereas the highest ( $p < 0.05$ ) adsorption capacity of rutin was reached at pH 6. There was no significant difference observed between pH 6 and 11. However, quercetin gave the highest ( $p < 0.05$ ) adsorption capacity at pH 9 to 11.

Although there was a similar trend of adsorption capacity for these three phenolic compounds, the pH where maximum adsorption capacity achieved was different from each of them. According to Altiok et al. [38], the results might be different from other phenolic compounds as phenolic profile varies in their molecular sizes and forms which influence their solubility and adsorption. As the value of pH increase, adsorption capacities of phenolic compounds also increase. It might happen due to the decrease in competition between the charged ions for the same functional group of the resin used. A change of the  $H_3O^+$  concentration in the solution resulted changes in the ratio of protonated/unprotonated polyphenolic compounds. Protonation of these polyphenolic compounds significantly change their charges as well as the affinity to negatively charged adsorption resin Amberlite IRA 67 [39].

Based on the results, noni juice treated with weak base anion exchange resin (Amberlite IRA 67) showed promising potential in octanoic and hexanoic acid removal while it also minimize the loss of antioxidants at specific pH. Haslaniza et al. [4, 11] also reported that noni juice treated with the same resin is good to be used for deodorization due to lower reduction on antioxidant content compared to other resins.

#### 4. Conclusion

Based on the model system, it shows adsorption onto Amberlite IRA 67 was influenced by the initial concentration of each compound. The removal of both organic acids and phenolic compounds was shown to be dependent on phase contact time and initial concentration. The initial concentration influences the adsorption kinetics of each compound studied. Also, the values of initial adsorption rate,  $1/K_1$ , and adsorption extent,  $1/K_2$ , decreased with the increase of initial concentration for both organic acids and phenolic compounds. As for the isotherm model, the results for all the compounds studied fitted well to the Langmuir model as a monolayer sorption. The Langmuir model suggests a higher adsorption affinity of the phenolic compounds compared to both organic acids. Based on the adsorption characteristics, no differences were observed that could differentiate the adsorption between organic acids and phenolic compounds. Thus, further studies are needed to be able to differentiate and subsequently maximize organic

acids adsorption while minimizing phenolic compounds reduction. Based on the results, noni juice treated with weak base anion exchange resin (Amberlite IRA 67) showed promising potential in octanoic and hexanoic acid removal while it also minimizes the loss of antioxidants at specific pH.

#### Data Availability

The data used to support the findings of this study are available from the corresponding author upon request.

#### Conflicts of Interest

The authors declare that there are no conflicts of interest regarding the publication of this paper.

#### Acknowledgments

The authors would like to thank the Ministry of Education (MOE) for the scholarship, Ministry of Science, Technology and Innovation (MOSTI) for financing the project under Grant ERGS/1/2013/STWN03/UKM/02/1, and Universiti Kebangsaan Malaysia, Bangi, Selangor, Malaysia.

#### References

- [1] European Commission, Scientific Committee of Food, *Opinion of the Scientific Committee on Food of Tahitian Noni Juice*. SCF/CS/DOS/18 ADD 2, European Commission, Brussels, Belgium, 2002.
- [2] H. Norma, A. Normah, A. W. Ahmad, M. Y. Rohani, M. Muhammad Gawas, and A. Sharizan, "Reducing the smelly compounds (caproic, caprylic and capric acids) in noni by treating the juice with activated charcoal powder," in *Proceedings of the National Food Technology Seminar*, Malaysia, 2004.
- [3] E. Vera, M. Dornier, J. Ruales, F. Vaillant, and M. Reynes, "Comparison between different ion exchange resins for the deacidification of passion fruit juice," *Journal of Food Engineering*, vol. 57, no. 2, pp. 89–96, 2003.
- [4] H. Haslaniza, W. A. Wan Yaacob, H. Osman, and M. Y. Maskat, "Interaction of antioxidants and organic acid from noni (*Morinda citrifolia* L.) juice with ion exchange resins during deodorization via deacidification," *Der Pharma Chemica*, vol. 7, no. 9, pp. 9–21, 2015.
- [5] Z. M. Zin, A. A. Hamid, A. Osman, and N. Saari, "Antioxidative activities of chromatographic fractions obtained from root, fruit and leaf of Mengkudu (*Morinda citrifolia* L.)," *Food Chemistry*, vol. 94, no. 2, pp. 169–178, 2006.
- [6] V. Maharaj and C. K. Sankat, "Rehydration characteristics and quality of dehydrated dasheen leaves," *Canadian Agricultural Engineering*, vol. 42, pp. 81–85, 2000.
- [7] P. A. Sopade and K. Kaimur, "Application of Peleg's equation in desorption studies of food systems: a case study with sago (*Metroxylon Sagu* rottb.) starch," *Drying Technology*, vol. 17, no. 4-5, pp. 975–989, 1999.
- [8] E. Palou, A. Lopez-Malo, A. Argaiz, and J. Welti, "Use of Peleg's equation to osmotic concentration of papaya," *Drying Technology*, vol. 12, no. 4, pp. 965–978, 1994.
- [9] M. M. Poojary and P. Passamonti, "Extraction of lycopene from tomato processing waste: kinetics and modelling," *Food Chemistry*, vol. 173, pp. 943–950, 2015.

- [10] S. Deng, B. J. West, and C. J. Jensen, "A quantitative comparison of phytochemical components in global noni fruits and their commercial products," *Food Chemistry*, vol. 122, no. 1, pp. 267–270, 2010.
- [11] H. Haslaniza, W. A. Wan Yaacob, S. I. Zubairi, and M. Y. Maskat, "Potential of Amberlite IRA 67 resin for deacidification of organic acids in noni juice," *Der Pharma Chemica*, vol. 7, no. 12, pp. 62–69, 2015.
- [12] M. Turhan, S. Sayar, and S. Gunasekaran, "Application of Peleg model to study water absorption in chickpea during soaking," *Journal of Food Engineering*, vol. 53, no. 2, pp. 153–159, 2002.
- [13] F. N. M. Fazil, N. S. M. Azzimia, B. H. Yahaya, N. A. Kamalaldin, and S. I. Zubairi, "Kinetics extraction modelling and antiproliferative activity of *Clinacanthus nutans* water extract," *The Scientific World Journal*, vol. 2016, Article ID 7370536, 7 pages, 2016.
- [14] Z. S. Othman, N. S. Hasan, and S. I. Zubairi, "Response surface optimization of rotenone using natural alcohol-based deep eutectic solvent as additive in the extraction medium cocktail," *Journal of Chemistry*, vol. 2017, Article ID 9434168, 10 pages, 2017.
- [15] M. Peleg, "An empirical model for the description of moisture sorption curves," *Journal of Food Sciences*, vol. 53, no. 4, pp. 1216–1219, 1988.
- [16] Y. Noor Hafizah, *Kesan Penyahasidan Terhadap Ciri-Ciri Ekstrak Mengkudu (Morinda citrifolia L.)*, M.S. thesis, Universiti Kebangsaan Malaysia, Bangi, Selangor, Malaysia, 2011.
- [17] C. G. Zambonin, M. Quinto, N. De Vietro, and F. Palmisano, "Solid-phase microextraction–gas chromatography mass spectrometry: a fast and simple screening method for the assessment of organophosphorus pesticides residues in wine and fruit juices," *Food Chemistry*, vol. 86, no. 2, pp. 269–274, 2004.
- [18] M. Wawrzekiewicz and Z. Hubicki, "Equilibrium and kinetic studies on the adsorption of acidic dye by the gel anion exchanger," *Journal of Hazardous Materials*, vol. 172, no. 2-3, pp. 868–874, 2009.
- [19] H. Yuh-Shan, "Isotherms for the sorption of lead onto peat: comparison of linear and non-linear methods," *Polish Journal of Environmental Studies*, vol. 15, no. 1, pp. 81–86, 2006.
- [20] A. Mittal, D. Kaur, and J. Mittal, "Batch and bulk removal of a triarylmethane dye, Fast Green FCF, from wastewater by adsorption over waste materials," *Journal of Hazardous Materials*, vol. 163, no. 2-3, pp. 568–577, 2009.
- [21] R. L. Johnson and B. V. Chandler, "Reduction of bitterness and acidity in grape fruit juice by adsorption processes," *Journal of Science and Food Agricultural*, vol. 33, no. 3, pp. 287–293, 1982.
- [22] M. Hasnain Isa, L. S. Lang, F. A. H. Asaari, H. A. Aziz, N. Azam Ramli, and J. P. A. Dhas, "Low cost removal of disperse dyes from aqueous solution using palm ash," *Dyes and Pigments*, vol. 74, pp. 446–453, 2007.
- [23] Y. S. Yien, O. Hassan, and S. I. Zubairi, "Deodorizing mechanism of  $\beta$ -cyclodextrin-organic acids inclusion against strong odor of *Morinda Citrifolia* (Mengkudu) juice," *Jurnal Teknologi*, vol. 79, no. 10, pp. 67–75, 2016.
- [24] G. Pineiro, S. Perelman, J. P. Guerschman, and J. M. Paruelo, "How to evaluate models: observed vs. predicted or predicted vs. observed?," *Ecological Modelling*, vol. 216, no. 3-4, pp. 316–322, 2008.
- [25] S. S. Mariam, Y. Yamin, and H. Zaini, "Adsorption of anionic amido black dye by layered double hydroxide, ZnAlCO<sub>3</sub>-LDH," *The Malaysian Journal of Analytical Sciences*, vol. 13, no. 1, pp. 120–128, 2009.
- [26] N. K. Amin, "Removal of reactive dye from aqueous solutions by adsorption onto activated carbons prepared from sugarcane bagasse pith," *Desalination*, vol. 223, no. 1–3, pp. 152–161, 2008.
- [27] N. Kannan and M. M. Sundaram, "Kinetics and mechanism of removal of methylene blue by adsorption on various carbons—a comparative study," *Dyes and Pigments*, vol. 51, no. 1, pp. 25–40, 2001.
- [28] M. Ozacar and A. I. Sengil, "Adsorption of metal complex dyes from aqueous solutions by pine sawdust," *Bioresource Technology*, vol. 96, no. 7, pp. 791–795, 2005.
- [29] K. J. Gauraj, J. A. Farhan, and K. K. Roop, *Theory and Practice of Physical Pharmacy*, Elsevier, Haryana, India, 2012.
- [30] M. Carmona, A. Lucas, J. Valverde, B. Velasco, and J. Rodriguez, "Combined adsorption and ion exchange equilibrium of phenol on Amberlite IRA-420," *Chemical Engineering Journal*, vol. 117, no. 2, pp. 155–160, 2006.
- [31] X. Geng, P. Ren, G. Pi, R. Shi, Z. Yuan, and C. Wang, "High selective purification of flavonoids from natural plants based on polymeric adsorbent with hydrogen-bonding interaction," *Journal of Chromatography A*, vol. 1216, no. 47, pp. 8331–8338, 2009.
- [32] M. Parsaei and M. S. Goodarzi, "Adsorption study for removal of boron using ion exchange resin in batch system," *International Conference on Environmental Sciences and Technology IPCBEE*, vol. 6, pp. 398–402, Singapore, February 2011.
- [33] O. S. Amuda and A. O. Ibrahim, "Industrial wastewater treatment using natural material as adsorbent," *African Journal of Biotechnology*, vol. 5, no. 16, pp. 1483–1487, 2006.
- [34] S. Ghorai and K. K. Pant, "Investigations on the column performance of fluoride adsorption by activated alumina in a fixed-bed," *Chemical Engineering Journal*, vol. 98, no. 1-2, pp. 165–173, 2004.
- [35] A. M. B. Hamissa, M. C. Ncibi, B. Mahjoub, and M. Seffen, "Biosorption of metal dye from aqueous solution onto Agave Americana (L.) fibres," *International Journal of Environmental Science and Technology*, vol. 5, no. 4, pp. 501–508, 2008.
- [36] M. Greluk and Z. Hubicki, "Comparison of the gel anion exchangers for removal of acid orange 7 from aqueous solution," *Chemical Engineering Journal*, vol. 170, no. 1, pp. 184–193, 2011.
- [37] Y. Berbar, M. Amara, and H. Kerdjoudj, "Effect of adsorption of polyethyleneimine on the behaviour of anion exchange resin," *Procedia Engineering*, vol. 33, pp. 126–133, 2012.
- [38] E. Altioek, D. Baycin, O. Bayraktar, and S. Ulku, "Isolation of polyphenols from the extracts of olive leaves by adsorption on silk fibroin," *Separation and Purification Technology*, vol. 62, no. 2, pp. 342–348, 2008.
- [39] D. R. Kammerer, Z. H. Saleh, R. Carle, and R. A. Stanley, "Adsorptive recovery of phenolic compounds from apple juice," *European Food Research & Technology*, vol. 224, no. 5, pp. 605–613, 2007.



Hindawi

Submit your manuscripts at  
[www.hindawi.com](http://www.hindawi.com)

